

# WIDEBAND ARRAY PROCESSING ALGORITHMS FOR ACOUSTIC TRACKING OF GROUND VEHICLES

Tien Pham and Brian M. Sadler  
U. S. Army Research Laboratory  
Adelphi, MD 20783-1197  
tpham@arl.mil

## Abstract

Focused wideband adaptive array processing algorithms are used for the high-resolution aeroacoustic direction-finding of ground vehicles. Methods based on coherent focusing such as steered covariance matrix (STCM), and spatial smoothing or interpolation using the array manifold interpolation (AMI) method, will be discussed [1, 2]. Experimental results for a circular array are presented comparing and contrasting the coherent focused wideband methods with the incoherent wideband methods. Detailed analysis of the incoherent wideband MUSIC (IWM) algorithm versus the focused or coherent wideband MUSIC (CWM) algorithms shows processing gain over narrowband MUSIC in terms of accuracy and stability of the direction of arrival (DOA) estimates [3]. Given adequate SNR, incoherent wideband methods yield more accurate DOA estimates than focused methods for highly peaked spectra. On the other hand, the coherent wideband methods yield better DOA estimates for sources with flat spectra [4]. In general, the focused wideband methods are much more statistically stable than the incoherent wideband methods. In this paper, experimental results are shown for IWM, ICM, and AMI uniform circular array MUSIC (AMI-UCA MUSIC) algorithms using acoustic data collected from a 12-element UCA and computational complexity is discussed.

## 1. Introduction

This paper describes work at the Army Research Laboratory (ARL) on array signal processing algorithms using small baseline acoustic arrays to passively detect, estimate direction of arrival (DOA), track, and classify moving targets for implementation in an acoustic sensor testbed [5]. The acoustic detection and tracking of ground vehicles in a battlefield environment is a very challenging problem because ground vehicle acoustic signatures are wideband and nonstationary. Atmospheric effects and wind noise limit the range of detection and useful signal content to the frequency range of 20 to 200 Hz. The small array baselines are physically constrained by system requirements and lack of spatial coherence; therefore, conventional beamforming techniques provide poor spatial resolution, motivating the use of adaptive high-resolution DOA algorithms. By exploiting the multi-spectral content of the ground targets, processing gain is obtained through wideband processing.

Current efforts are focused on wideband signal subspace DOA algorithms, such as wideband MUSIC. Validation is accomplished using experimental data, and successful algorithms are implemented in the acoustic sensor testbed. Experimental results using a circular array of six sensors (plus 1 at the array center), with a diameter of 8 ft has been presented in [3, 4, 6]. Both the incoherent wideband MUSIC (IWM) and coherent wideband MUSIC (CWM) algorithms provide processing gain over narrowband MUSIC, as shown by experimental analysis. Given adequate SNR, IWM performs well and yields sharp and distinct peaks in the beampattern. However, frequency selection is an issue, because the inclusion of low SNR frequency bins tends to degrade the resulting beampattern, reducing source peaks and introducing spurious peaks. In contrast, the coherent MUSIC approach is much more statistically stable, with a beampattern that generally improves with the addition of lower SNR bins. However, inclusion of more frequency bins can introduce bias errors. The coherent approach outperforms the incoherent in terms of DOA accuracy with sources that have relatively flat spectra. Conversely, for sources with highly peaked spectra the incoherent approach yields better DOA results. In general, the coherent focused wideband methods are much more statistically stable than any of the incoherent wideband methods but at higher computational cost. We also note that coherent processing has great practical importance because it can handle fully correlated signals (e.g., multipath).

Computational complexity is an issue when considering implementation of any real-time algorithm into the acoustic sensor testbed. Here real-time implies updates roughly every second or less. Coherent methods such as the steered covariance matrix (STCM) combine the narrowband cross-spectral density matrices (CSDM) into one focused CSDM at each look direction. The look-direction dependency increases the computational complexity unless there are

preliminary source location estimates, e.g., from a priori knowledge or from a coarse beamformer. Spatial interpolation is a more computationally efficient coherent wideband focusing method that accurately focuses arrivals from all directions simultaneously. Recent work by Doron and others has extended spatial interpolation to circular and other arbitrary array configurations. Doron's method is called array manifold interpolation (AMI) [2, 7]. For our application, based on the radius of the uniform circular array (UCA) of 4 ft, and a maximum frequency of interest of 200 Hz, the number of sensors needed to apply AMI is roughly 12 or more. During a field experiment in July 1997 at the Spesutie Island test site, Aberdeen Proving Ground (APG), Maryland, we utilized a UCA of 12 sensors with a 4 ft radius, and collected acoustic signatures of moving ground vehicles traveling from ranges of 50 m to beyond 1 km.

In this paper, we will discuss the algorithm formulations and present experimental results with the 12 sensor UCA comparing and contrasting STCM and AMI. We apply MUSIC on the focused CSDM to obtain beampatterns. GPS ground truth was not available for the data collected, so a qualitative analysis is provided based on beampattern sharpness. Where appropriate, we will compare both coherent algorithms (CWM and AMI-UCA MUSIC) to the incoherent algorithm (IWM).

## 2. Algorithm Formulations

In acoustic wideband processing, we exploit the multi-spectral content of the acoustic signature. Ideally, we would like to use the entire frequency spectrum of the signal. In practice, due to atmospheric effects and wind noise, most of the relevant acoustic signal power lies within the frequency range  $B_f = [20, 200]$  Hz. For this frequency range, the bandwidth is  $BW = 180$  Hz, with a center frequency is  $f_c = 110$  Hz. When applying super-resolution DOA techniques, it is desirable to have  $BW \lesssim 0.1f_c$ , which is clearly not the case for our problem. The coherent wideband methods described in the following for UCAs do not theoretically require that  $BW \lesssim 0.1f_c$ . However, we observe through simulation and experimental analysis that in the case of spatial interpolation the performance degrades for  $BW$  large compared to  $f_c$  because the signal subspaces do not align well.

In coherent wideband processing for direction-finding, we coherently combine  $M$  (the number of narrowband frequency components) CSDMs into one focused CSDM, and then perform high resolution direction-finding (such as MUSIC) on the focused CSDM. The following describes the steps to compute the narrowband CSDMs: (1) obtain sampled data  $y_i(t)$  for each sensor  $i$ ,  $i = 1, 2, \dots, N$ , where  $N$  is the number of sensor elements in the array; (2) compute  $Y_i(f) = DFT\{y_i(t)\}$ ,  $\forall i$ , the discrete Fourier transform (DFT) of  $y_i(t)$ ; (3) apply a spectral peak picker to select the  $M$  narrowband frequency components  $f_m \in B_f$  for  $m = 1, 2, \dots, M$ ; and (4) compute the estimated CSDM  $\hat{R}_Y(f_m) = \hat{Y}(f_m)^H \hat{Y}(f_m)$ ,  $\forall f_m$ , where  $\hat{Y}(f_m) = [Y_1(f_m), Y_2(f_m), \dots, Y_N(f_m)]^T$ . The estimated narrowband CSDMs are then focused over  $f_m \in B_f$  to form a representative focused CSDM.

### 2.1. Steered Covariance Matrix

The STCM algorithm was originated by Wang and Kaveh [1, 8]. STCM is based on forming the composite or focused CSDM given by

$$\hat{R}_{focus}(\mathbf{q}) = \sum_{m=1}^M T(f_m, \mathbf{q}) \hat{R}_Y(f_m) T(f_m, \mathbf{q})^H. \quad (1)$$

The steering or focusing matrix,  $T(f_m, \mathbf{q})$ , is a function of both frequency,  $f_m$ , and look direction or angle,  $\mathbf{q}$ . Here it is defined as the  $N \times N$  diagonal matrix:

$$T(f_m, \mathbf{q}) = \text{diag}\left[e^{2j\mathbf{p}_m^T \Delta \mathbf{f}_1}, e^{2j\mathbf{p}_m^T \Delta \mathbf{f}_2}, \dots, e^{2j\mathbf{p}_m^T \Delta \mathbf{f}_N}\right], \quad (2)$$

where  $\Delta \mathbf{f}_i = r/c \sin \mathbf{f}_i$ ,  $\mathbf{f}_i = \mathbf{a}_i - (90 - \mathbf{q})$ ,  $\mathbf{a}_i$  is the angle relative to the normal for sensor  $i$ ,  $r$  is the radius of the circular array, and  $c$  is the speed of sound in air. The resulting STCM,  $\hat{R}_{focus}(\mathbf{q})$ , focuses a signal in the respective narrowband cross-spectral density into the same subspace, yielding coherent processing gain over multiple frequencies. Conventional

subspace methods can then be applied to  $\hat{R}_{focus}(\mathbf{q})$ . Work at ARL has provided detailed description of the application of MUSIC to  $\hat{R}_{focus}(\mathbf{q})$  [3, 4].

## 2.2. Array Manifold Interpolation

Spatial smoothing or interpolation for uniform linear arrays was first introduced by Evans *et. al.* [9] and further developed by others [1, 10, 11]. Doron introduced spatial interpolation (i.e., AMI) for wideband array processing for an arbitrary two-dimensional array with known geometry for direction-finding [2, 7]. The AMI algorithm transforms the array manifolds at frequencies  $f_m \in B_f$  so that they can be aligned and averaged into a single array manifold at a focus frequency  $f_o$ . The transformation is done using the series expansion of a plane wave in polar coordinates, where each term in the expansion is a function of  $J_n(\cdot)$ , the  $n^{\text{th}}$  order Bessel functions of the first kind. To apply AMI, which approximates the series expansion by truncation, the condition

$$|J_n(k_{\max}r_{\max})| < \mathbf{e}, \text{ for } n > n_e \quad (3)$$

must be met for some small number  $\mathbf{e}$ , where  $k_{\max} = 2\mathbf{p}f_{\max}/c$  is the maximum wave number in  $B_f$ , and  $r_{\max}$  is the maximum sensor distance from a reference origin. This condition is based on the fact that for  $n \gg kr$ , the Bessel function  $J_n(kr)$  decreases faster than the exponential function, and in fact, the decay of the Bessel function begins when the order of Bessel function is equal to its argument. Equation (3) leads to an equivalent condition; that is the number of sensors in the array obeys  $N \geq 2n_e$ . We apply the AMI algorithm to UCA (AMI-UCA) for coherent wideband processing and then apply MUSIC for direction-finding.

The coherently combined or focused CSDM for the AMI-UCA is defined as [2, 7]

$$\hat{R}_{focus} = \sum_{m=1}^M T_m \hat{R}_Y(f_m) T_m^H = F \left[ \sum_{m=1}^M D(k_m) F^H \hat{R}_Y(f_m) F D(k_m)^H \right] F^H, \quad (4)$$

where the transformation matrix  $T_m = F D(k_m) F_m^{-1}$ ,  $F$  is a unitary  $N \times 2n_e$  matrix (we use  $2n_e = N$ ) whose elements are

$$F_{nl} = \exp\left\{-j \frac{2\mathbf{p}nl}{N}\right\}, \text{ for } n = 0, 1, \dots, N-1; l = -n_e + 1, \dots, n_e; \quad (5)$$

and  $D(k_m)$  is a diagonal matrix whose main diagonal elements are the scaling factors

$$[D(k_m)]_{mm} = \frac{J_n(k_o r)}{J_n(k_m r)}, \quad (6)$$

where  $k_m$  and  $k_o$  are the corresponding wave numbers for  $f_m$  and  $f_o$ , respectively. The right-hand side of equation (4) can be efficiently computed using a DFT followed by a simple scaling calculation. In fact, given  $N$ ,  $B_f$  and  $f_o$ ,  $D(k_m)$  and  $F$  can be pre-computed and stored in a look-up table. Unlike the STCM in equation (1),  $\hat{R}_{focus}$  for AMI in equation (4) is not a function of the look angle and, therefore, only needs to be computed once for all look directions.

## 3. Experimental Results

Table 1 shows the minimum  $N$  that satisfies equation (3) for  $\mathbf{e} = 0.04, 0.01, 0.001$ ;  $r_{\max} = r = 4$  ft (radius of the UCA); and  $f_{\max} = 50, 100, 150, 200$  Hz. To do spatial interpolation, there must be a sufficient number of spatial data points (i.e., sensors) for interpolation to work accurately. Based on the calculations in table 1 for a 12-element UCA with a  $r = 4$  ft and  $\mathbf{e} = 0.04$ , we should apply the AMI-UCA algorithm to acoustic signatures in the frequency range  $B_f = [20, 150]$  Hz. A spectrogram of a typical tank recording is shown in figure 1. The tank was traveling at a constant speed of 20 mph while it was maneuvering around the Spesutie Island test site. We observe that most of the spectral content is below 200 Hz except around the closest point of approach (CPA), a distance of roughly 50 m, which is approximately [50, 80] s. Also, wind noise tends to dominate the signature below 20 Hz. Applying the wideband algorithms to the frequency range  $B_f = [20, 150]$  Hz will exploit most of the acoustic energy emitted.

Figure 2 shows the beampatterns versus time for (a) IWM, (b) CWM, and (c) AMI-UCA MUSIC algorithms for the experimental test run shown in figure 1. Wideband processing is over  $B_f = [20,150]$  Hz using a peak picker that selects up to  $M = 20$  spectral peaks based on a spectral threshold. For the AMI-UCA MUSIC algorithm, we used  $f_o = f_c = 85$  Hz, the center frequency of  $B_f$ . We see that IWM and CWM algorithms produce resulting beampatterns showing the DOA history of the tank as expected, while AMI-UCA MUSIC fails to produce any noticeable pattern. In this case, the poor performance of AMI-UCA MUSIC can be directly attributed to the fact that the condition  $BW \lesssim 0.1f_c$  is violated. We also observe through simulation that shows that the performance of AMI degrades as  $BW$  increases with respect to  $f_c$ .

We repeated the same experimental analysis for AMI-UCA MUSIC for a fixed  $BW = 20$  Hz and  $f_o = f_c$  for  $B_f = [40,60],[90,110],[140,160]$  Hz, and the results are shown in figure 3 (a), (b) and (c), respectively. We chose  $BW = 20$  Hz to make sure that  $BW < f_c$ , and that the respective  $B_f$  would include at least one of the engine harmonic lines. For each  $B_f$ , we can observe the beampatterns of the moving tank. The AMI-UCA MUSIC algorithm produces the best results for  $B_f = [90, 110]$  Hz. This is probably true for two reasons: (1)  $B_f = [90,110]$  Hz satisfies the conditions in equation (3) and  $BW \lesssim 0.1f_c$ , and (2)  $B_f = [90,110]$  Hz contains high SNR frequency components. Figure 4 shows the beampatterns versus time for (a) IWM, (b) CWM, and (c) AMI-UCA MUSIC algorithms for  $B_f = [90,110]$  Hz and  $f_o = f_c = 100$  Hz. We obtain the expected results for IWM and CWM. In this comparison of the wideband methods, AMI is not only the fastest but it also performs the best in term of sharpness of the resulting beampatterns.

We have shown that in general AMI-UCA is a more computationally efficient than STCM. When we combine the wideband processing with the MUSIC algorithm under certain parameters, AMI-UCA MUSIC is more computationally efficient than both IWM and CWM for each  $q = 1, \dots, 360$  and  $M = 20$  (i.e.,  $CWM > IWM \gtrsim$  AMI-UCA MUSIC in terms of complexity). The most expensive calculation involves singular value decomposition (SVD) which of order  $N^3$ . CWM requires one SVD calculation for each  $q$  (360 in all for 1 degree resolution), IWM requires one SVD calculation for each  $f_m$  ( $M$  frequency peaks), and AMI-UCA MUSIC requires one SVD total and the use of DFT for focusing in equation (4). See [3, 4, 6] for further details on complexity calculations for IWM and CWM.

## 4. Conclusions

In this paper, we have shown experimental results of wideband acoustic array processing methods developed at ARL for performing direction-finding and tracking of ground vehicles. Current work is focused on robust and low-complexity algorithms for the purpose of real-time implementation in an acoustic sensor testbed. We have shown previously that real-time results can be obtained using IWM and CWM [6], and here we compare those methods with a coherent wideband method based on spatial interpolation for uniform circular arrays (i.e., AMI-UCA). We combined AMI-UCA with the MUSIC algorithm and compared the resulting beampatterns of IWM and CWM. In general, for the frequency range of interest,  $B_f = [20,200]$  Hz, IWM and CWM perform well while AMI-UCA MUSIC breaks down. However, when we limited the frequency range to satisfy the conditions in equation (3) and  $BW \lesssim 0.1f_c$ , AMI-UCA MUSIC outperformed IWM and CWM in terms of beam sharpness in our experiments. Preliminary results are promising but further analysis is required to fully characterize the performance of AMI-UCA MUSIC. The computational complexity of AMI-UCA MUSIC is less than IWM under certain parameters, thus real-time implementation is possible.

## References

- [1] J. Krolik, "Focused wideband array processing for spatial spectral estimation," chapt. 6 in *Advances in Spectrum Analysis and Array Processing Vol. II*, S. Haykin ed., Prentice-Hall, 1991.
- [2] M. Doron, E. Doron and H. Weiss, "Coherent wide-band processing for arbitrary array geometry," *IEEE Trans. SP*, Vol. 41, No. 1, pp. 414-417, January 1993.

- [3] T. Pham and B. Sadler, "Adaptive wideband aeroacoustic array processing," *8th IEEE Statistic Signal and Array Processing Workshop*, pp. 295-298, Corfu, Greece, June 1996.
- [4] T. Pham and B. Sadler, "Wideband acoustic array processing to detect and track ground vehicles," *1<sup>st</sup> Annual ARL Sensors and Electron Devices Symposium*, pp. 151-154, College Park, MD, January 1997.
- [5] N. Srour and J. Robertson, "Remote Netted Acoustic Detection System: Final Report," ARL-TR-607, U. S. Army Research Laboratory, May 1995
- [6] T. Pham and M. Fong, "Real-time implementation of MUSIC for wideband acoustic detection and tracking," *SPIE AeroSense*, Orlando, FL, April 1997.
- [7] M. Doron and E. Doron, "Wavefield modeling and array processing, part I: spatial smoothing," *IEEE Trans. SP*, Vol. 42, No. 10, pp.2549-2559, April, 1994.
- [8] H. Wang and M. Kaveh, "Coherent signal-subspace processing for the detection and estimation of angles of arrival of multiple wideband sources," *IEEE Trans. ASSP*, Vol. 33, 823-831, August 1985.
- [9] J. Evans, J. Johnson, and D. Sun, "Application of advanced signal processing angle of arrival estimation in ATC navigation and surveillance systems," MIT Lincoln Lab., Lexington, MA, Rep. 582, 1982.
- [10] W. Du and R. Kirilin, "Improved spatial smoothing for DOA estimation of coherent signals," *IEEE Trans. Signal Processing*, vol.33, pp. 806-811, 1991.
- [11] B. Friedlander and A. Weiss, "Direction-finding using spatial smoothing with interpolated arrays," *IEEE Trans. Aerosp. Electron Syst.* vol. 28, no. 2 pp. 574-587, April 1992.

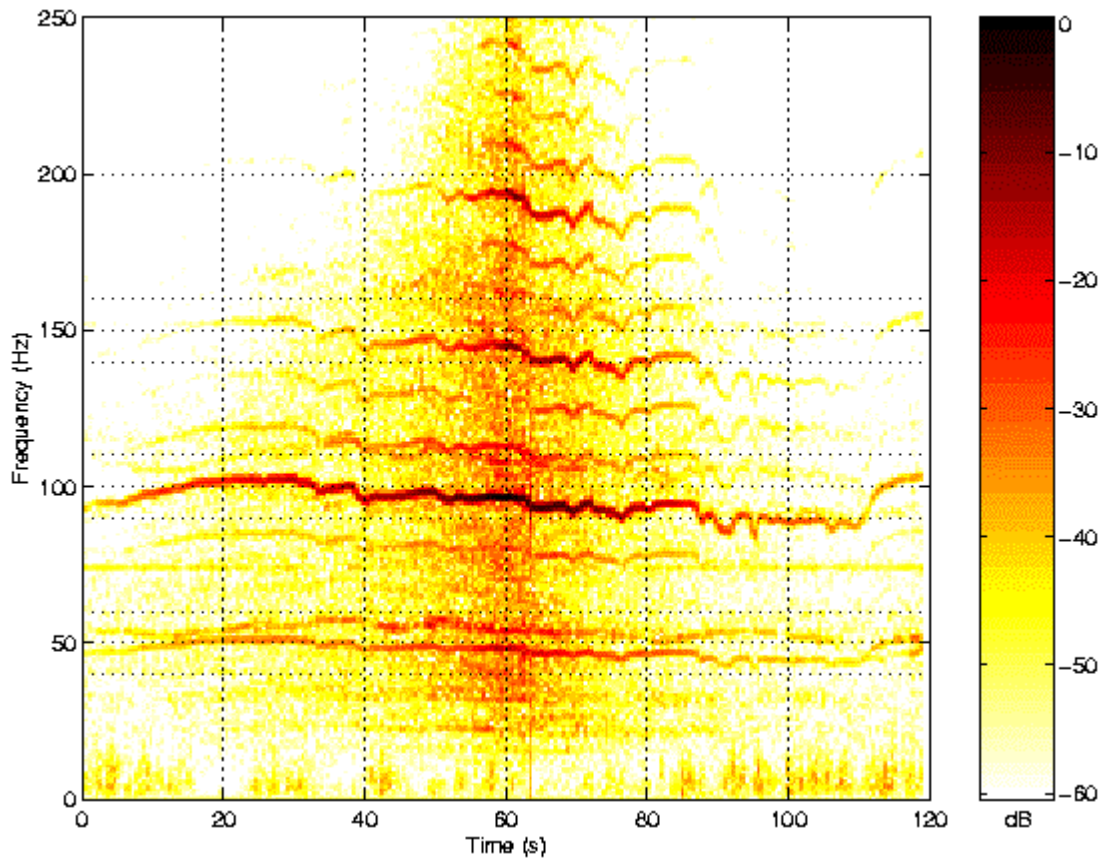


Figure 1: Spectrogram of a tank traveling at constant speed of 20 mph at Aberdeen Proving Ground (APG), MD.

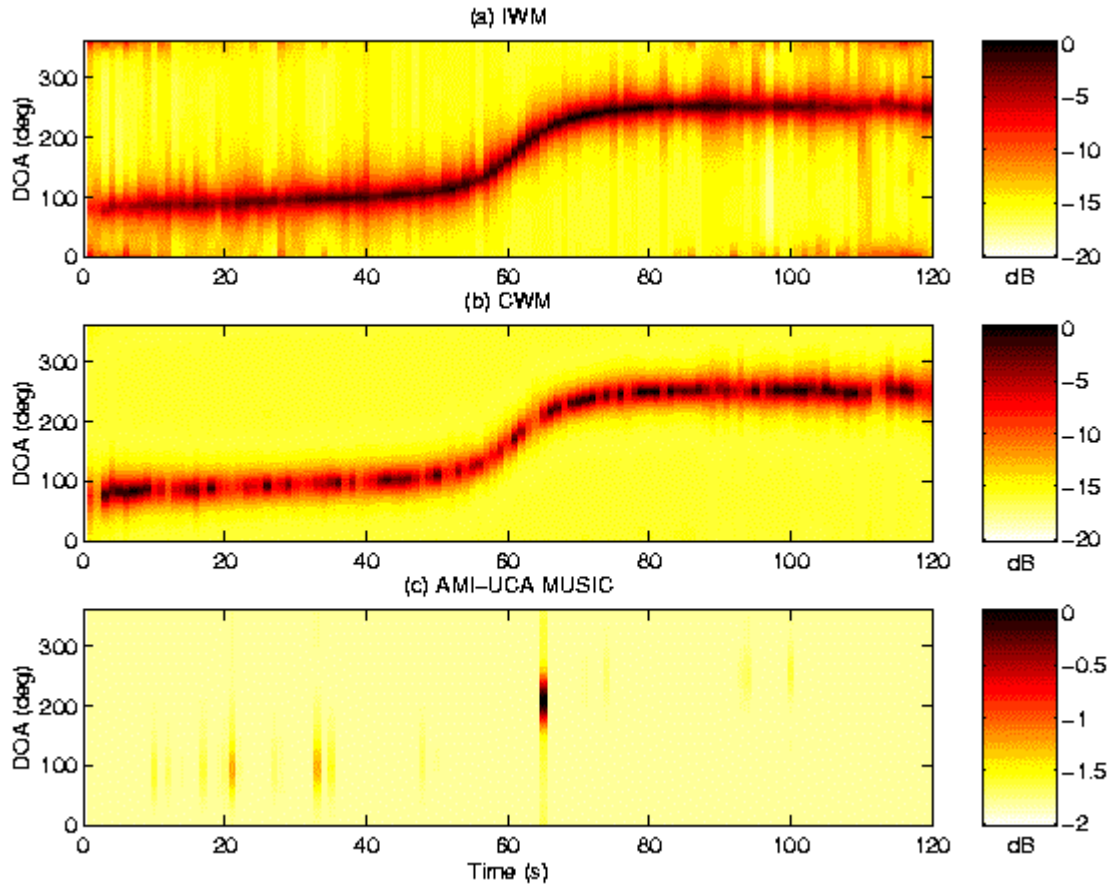


Figure 2: Beampatterns vs. time for three wideband algorithms (a) IWM, (b) CWM, and (c) AMI-UCA MUSIC for  $B_f = [20, 150]$  Hz and  $f_o = f_c = 85$  Hz.

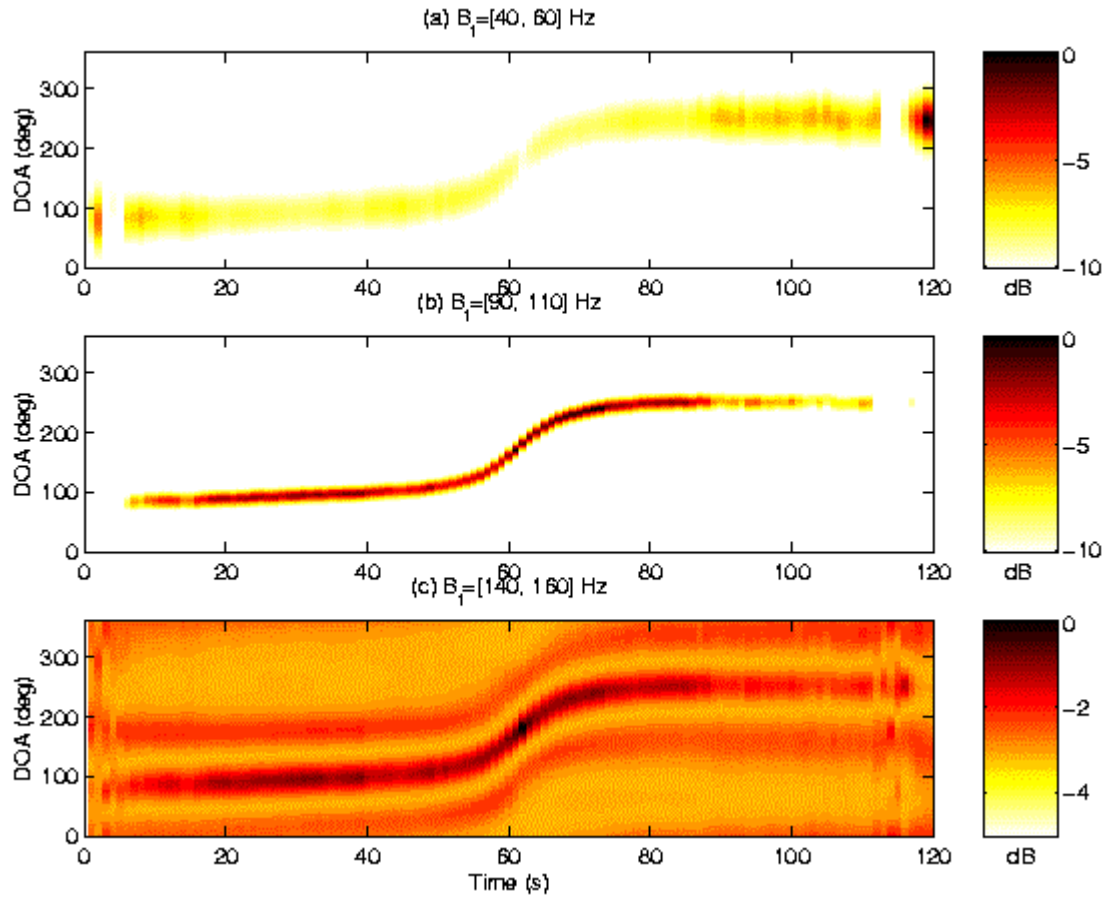


Figure 3: Beampatterns vs. time for AMI-UCA MUSIC algorithm for fixed  $BW = 20$  Hz with  $f_o = f_c$  for (a)  $B_f = [40, 60]$  Hz;  $f_o = 50$  Hz, (b)  $B_f = [90, 110]$  Hz,  $f_o = 100$  Hz; and (c)  $B_f = [140, 160]$  Hz.,  $f_o = 150$  Hz.

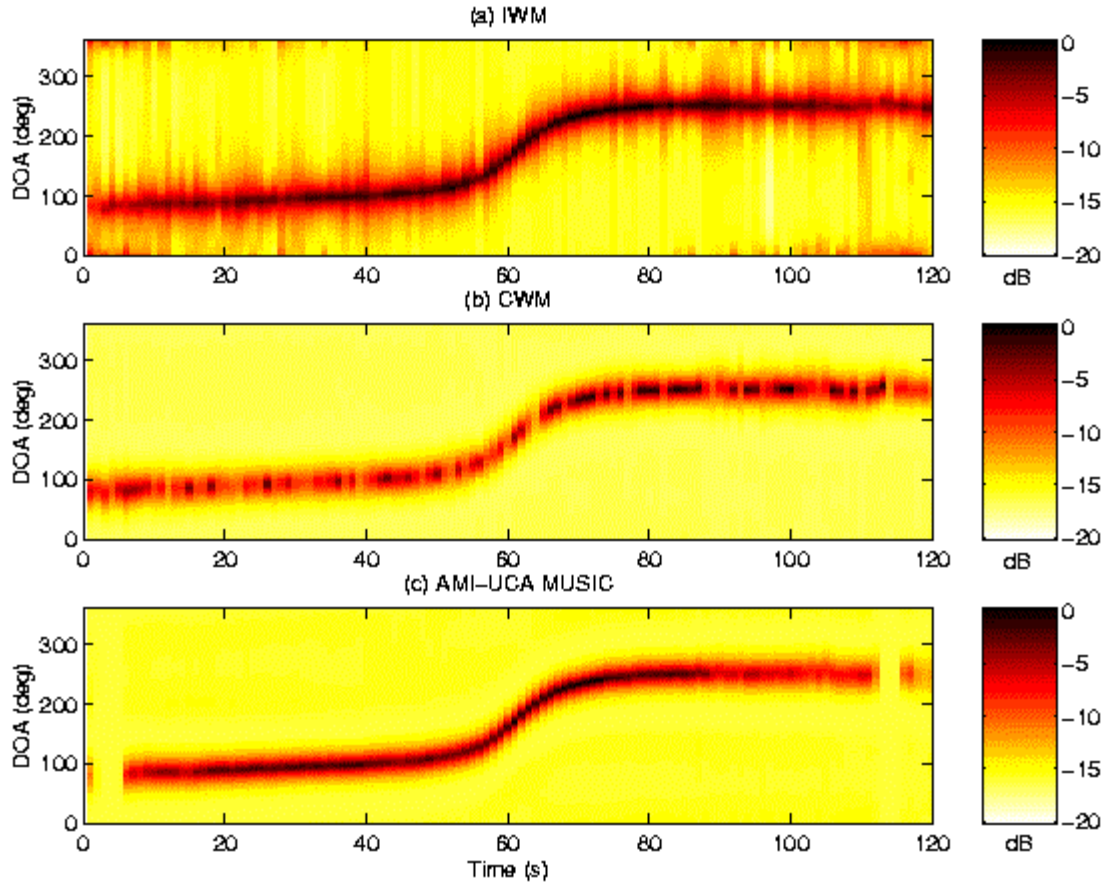


Figure 4: Beampatterns vs. time for (a) IWM, (b) CWM, and (c) AMI-UCA MUSIC algorithms for  $B_f = [90, 110]$  Hz and  $f_o = f_c = 100$  Hz.

$f_{\max}$ (Hz)	$N (e = 0.04)$	$N (e = 0.01)$	$N (e = 0.001)$
50	6	10	10
100	10	12	14
150	12	14	18
200	14	18	20

Table 1: Minimum number of sensors  $N$  that satisfy equation (3) for UCA of with radius 4 ft.

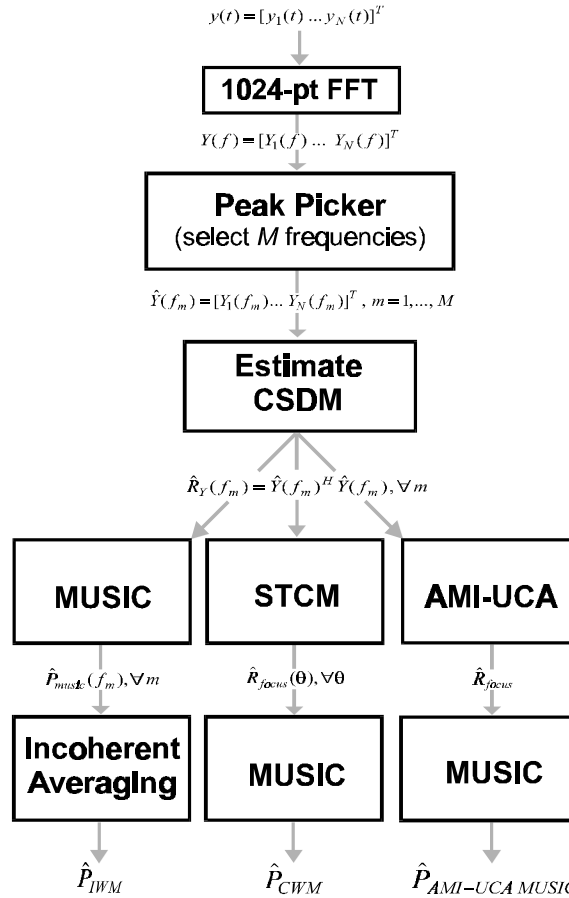
## Appendix

### Acronyms

AMI, Array Manifold Interpolation  
 AMI-UCA, AMI for Uniform Circular Array  
 APG, Aberdeen Proving Ground  
 ARL, Army Research Laboratory  
 CSDM, Cross Spectral Density Matrix  
 CWM, coherent wideband MUSIC  
 DFT, Discrete Fourier Transform  
 DOA, Direction of Arrival  
 IWM, incoherent wideband MUSIC  
 MUSIC, MUltiple SIgnal Characterization  
 SNR, Signal to Noise Ratio  
 STCM, STeered Covariance Matrix  
 UCA, Uniform Circular Array

### Notations and Variables

$\mathcal{B}_f$ , frequency band of interest  
 $BW$ , frequency bandwidth  
 $c$ , speed of sound in air  
 $f_o$ , focused frequency  
 $f_c$ , center frequency  
 $f_{\max}$ , maximum frequency in  $\mathcal{B}_f$   
 $J_n(\cdot)$ ,  $n^{\text{th}}$  order Bessel function of the first kind  
 $k_{\max}$ , maximum wave number corresponding to  $f_{\max}$   
 $k_o$ , focused wave number corresponding to  $f_o$   
 $M$ , number of frequency components  
 $N$ , number of sensor elements  
 $O(N^x)$ , computational complexity of order  $N^x$   
 $r$ , radius of UCA  
 $K_{focus}$ , focused CSDM  
 $\hat{R}_Y(f_m)$ , estimated CSDM at  $f_m$   
 $T(\cdot)$ , transformation or focusing matrix  
 $Y_i(f)$ , DFT of  $y_i(n)$   
 $y_i(t)$ , digitized output of sensor  $i$



Flow diagram of IWM, CWM and AMI-UCA MUSIC algorithms.